

**Supplementary information**

---

**Highly conducting single-molecule  
topological insulators based on mono- and  
di-radical cations**

---

In the format provided by the  
authors and unedited

# Supporting Information for:

## Highly conducting single-molecule topological insulators based on mono- and di-radical cations

Liang Li<sup>1,a</sup>, Jonathan Z. Low<sup>1,a</sup>, Jan Wilhelm<sup>b</sup>, Guanming Liao<sup>c</sup>, Suman Gunasekaran<sup>a</sup>, Claudia R. Prindle<sup>a</sup>, Rachel L. Starr<sup>a</sup>, Dorothea Golze<sup>d</sup>, Colin Nuckolls<sup>a</sup>, Michael L. Steigerwald<sup>a</sup>, Ferdinand Evers<sup>\*b</sup>, Luis M. Campos<sup>\*,a</sup>, Xiaodong Yin<sup>\*,c</sup>, Latha Venkataraman<sup>\*,a,e</sup>

<sup>1</sup>equal contribution

<sup>a</sup>Department of Chemistry, Columbia University, New York, New York 10027, United States

<sup>b</sup>Institute of Theoretical Physics, University of Regensburg, Regensburg, Germany

<sup>c</sup>Beijing Key Laboratory of Photoelectronic/Electrophotonic Conversion Materials, School of Chemistry and Chemical Engineering, Beijing Institute of Technology, Beijing, 102488 P. R. China

<sup>d</sup>Technische Universität Dresden, König-Bau, Bergstrasse 66 c, 01069 Dresden, Germany

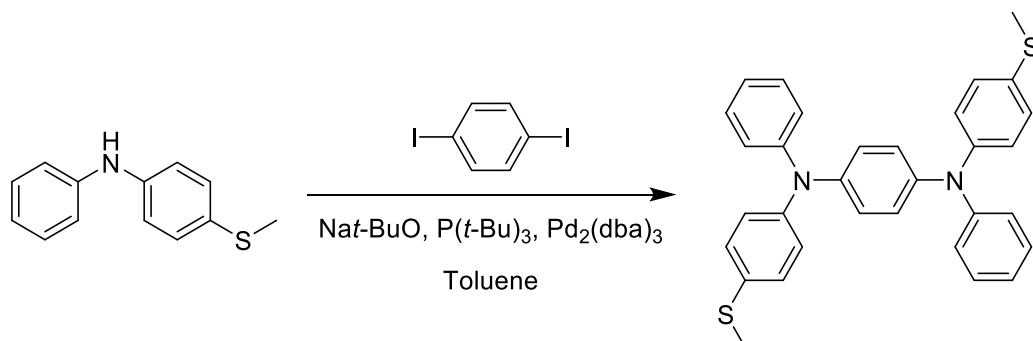
<sup>e</sup>Department of Applied Physics and Applied Mathematics, Columbia University, New York, New York 10027, United States

### Contents

1. Synthesis and Characterization	2
2. Oxidative Titration of Bis(triarylamine) Compounds	7
3. Additional Conductance Data	8
4. DFT calculations	14
5. NMR Spectra	21
6. References	28

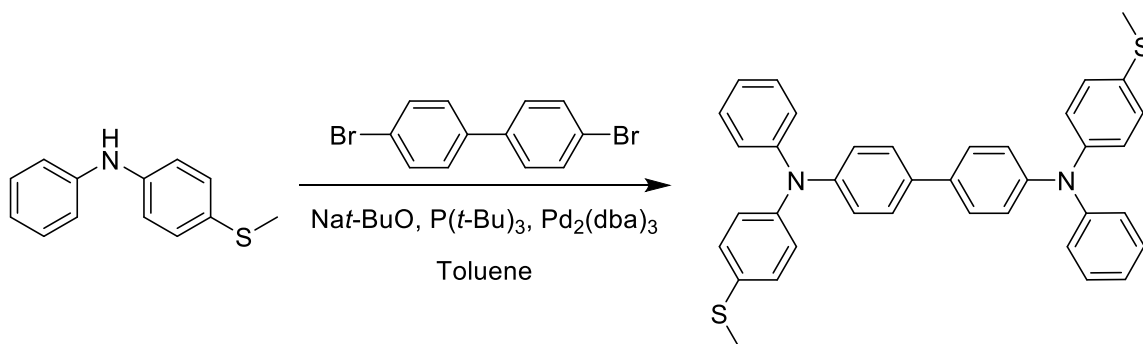
## 1. Synthesis and Characterization

### *N,N'*-bis(4-(methylthio)phenyl)-*N,N'*-diphenylbenzene-1,4-diamine (B1)



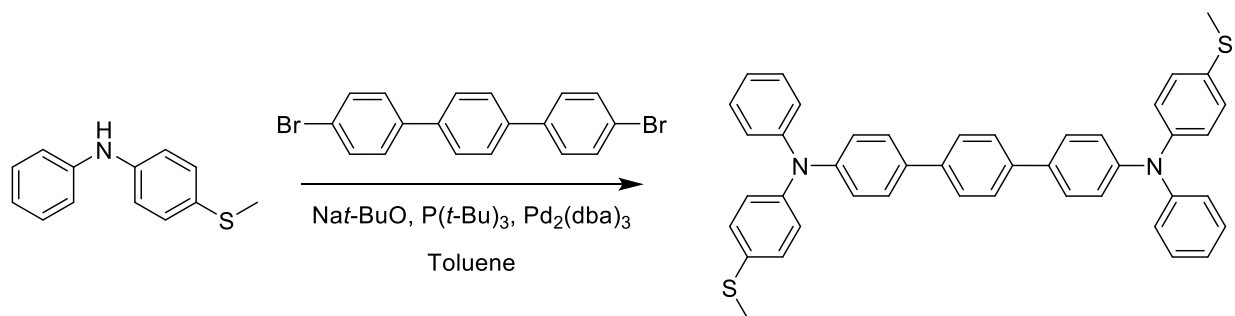
4-(methylthio)-*N*-phenylaniline (96mg, 0.45mmol), 1,4-diiodobenzene (74mg, 0.22mmol), and sodium *t*-butoxide (64mg, 0.67mmol) were charged into a 25mL Schlenk tube and 10mL toluene was added. After stirring 10 min under argon atmosphere, tri-*t*-butylphosphine (1M, 0.02mL) and tris(dibenzylideneacetone)dipalladium(0) (12mg, 0.013mmol) were added into the mixture in one portion. This mixture was kept stirring for 5h at room temperature, then washed with water and brine. The remaining organic phase was dried over sodium sulfate and all volatile components were removed on a rotary evaporator. Purification by column chromatography (silica gel, 25% DCM in hexanes as eluent) gave the product as white solid (60mg, 0.16mmol, 72%).  $^1\text{H-NMR}$  (400 MHz, Acetone- $d_6$ )  $\delta$  7.28 (dd,  $J = 8.5, 7.4$  Hz, 4H), 7.25 – 7.20 (m, 4H), 7.06 (dd,  $J = 8.6, 1.0$  Hz, 4H), 7.04 – 6.98 (m, 10H), 2.46 (s, 6H).  $^{13}\text{C-NMR}$  (126 MHz, Acetone- $d_6$ )  $\delta$  148.64, 146.39, 143.81, 132.74, 130.22, 129.18, 126.27, 125.18, 124.35, 123.51, 16.47. HRMS [ $\text{M}+\text{H}^+$ ]  $\text{C}_{32}\text{H}_{29}\text{N}_2\text{S}_2$  Calculated: 505.1772; Found: 505.1776.

### *N,N'*-bis(4-(methylthio)phenyl)-*N,N'*-diphenyl-[1,1'-biphenyl]-4,4'-diamine (B2)



4-(methylthio)-*N*-phenylaniline (200mg, 0.93 mmol), 4,4'-dibromo-1,1'-biphenyl (145mg, 0.46mmol), and sodium *t*-butoxide (134mg, 1.4 mmol) were charged into a 25mL Schlenk tube and 10mL toluene was added. After stirring 10 min under argon atmosphere, tri-*t*-butylphosphine (1M, 0.028mL) and tris(dibenzylideneacetone)dipalladium(0) (25mg, 0.028mmol) were added into the mixture in one portion. This mixture was kept stirring for 5h at room temperature then washed with water and brine. The remaining organic phase was dried over sodium sulfate, and all volatile components were removed on a rotary evaporator. Purification by column chromatography (silica gel, 25% DCM in hexanes as eluent) gave the product as white solid (150mg, 0.26mmol, 56.5%). <sup>1</sup>H-NMR (500 MHz, Acetone-d<sub>6</sub>) δ 7.60 – 7.55 (m, 4H), 7.32 (dd, *J* = 8.3, 7.5 Hz, 4H), 7.28 – 7.23 (m, 4H), 7.11 – 7.02 (m, 14H), 2.48 (s, 6H). <sup>13</sup>C-NMR (126 MHz, Acetone-d<sub>6</sub>) δ 147.58, 146.72, 145.24, 134.56, 132.48, 129.42, 128.19, 127.22, 124.92, 124.11, 123.73, 123.07, 15.46. HRMS [M+H<sup>+</sup>] C<sub>38</sub>H<sub>33</sub>N<sub>2</sub>S<sub>2</sub> Calculated: 581.2085; Found: 581.2084.

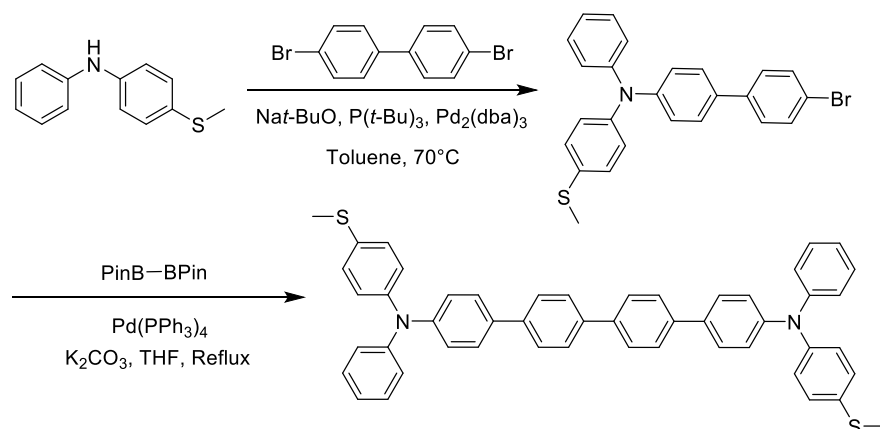
***N,N'*-bis(4-(methylthio)phenyl)-*N,N'*-diphenyl-[1,1':4',1''-terphenyl]-4,4''-diamine (B3)**



4-(methylthio)-*N*-phenylaniline (200mg, 0.93mmol), 4,4''-dibromo-1,1':4',1''-terphenyl (180mg, 0.46mmol), and sodium *t*-butoxide (134mg, 1.4mmol) were charged into a 25mL Schlenk tube and 10mL toluene was added. After stirring 10 min under argon atmosphere, tri-*t*-butylphosphine (1M, 0.028 mL) and tris(dibenzylideneacetone)dipalladium(0) (25mg, 0.028mmol) were added into the mixture in one portion. This mixture was stirred for 5h at room temperature, then washed with water and brine. The remaining organic phase was dried over sodium sulfate, and all volatile components were removed on a rotary evaporator. Purification by column chromatography (silica gel, 25% DCM in hexanes as eluent) gave the product as white solid (180mg, 0.273 mmol, 59.5%). <sup>1</sup>H-NMR (400 MHz, Acetone-d<sub>6</sub>) δ 7.74 (s, 4H), 7.69 – 7.62 (m, 4H), 7.33 (dd, *J* = 8.5, 7.4 Hz, 4H), 7.30 – 7.24 (m, 4H), 7.16 – 7.02 (m, 14H), 2.49 (s, 6H). <sup>13</sup>C-NMR (126 MHz, Acetone-d<sub>6</sub>) δ

148.44, 148.08, 146.08, 139.70, 135.27, 133.54, 130.35, 129.08, 128.38, 127.66, 125.96, 125.15, 124.46, 124.09, 16.33. HRMS  $[M+H^+]$   $C_{44}H_{37}N_2S_2$  Calculated: 657.2398; Found: 657.2391.

***N,N'''-bis(4-(methylthio)phenyl)-N,N'''-diphenyl-[1,1':4',1'':4'',1'''-quaterphenyl]-4,4'''-diamine (B4)***

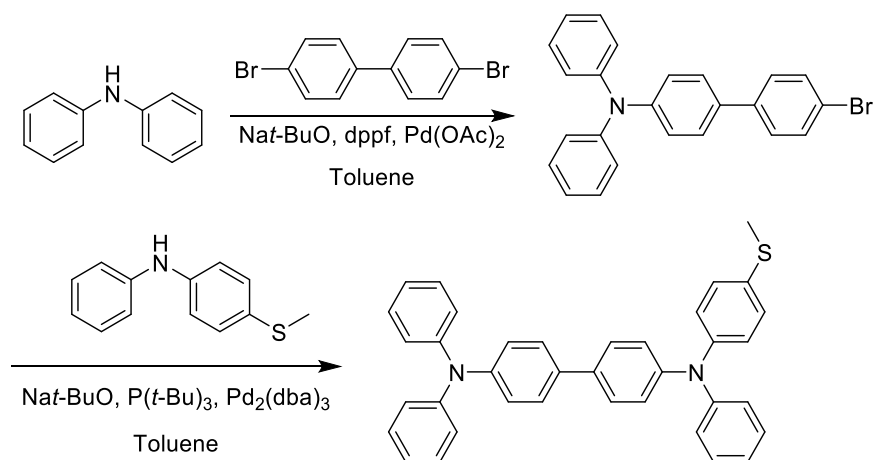


4-(methylthio)-*N*-phenylaniline (430mg, 2 mmol), 4,4'-dibromo-1,1'-biphenyl (618 mg, 2mmol), and sodium *t*-butoxide (288 mg, 3mmol) were charged into a 50 mL Schlenk tube and 20mL toluene was added. After stirring 10 min under argon atmosphere, tri-*t*-butylphosphine (1M, 0.12mL) and tris(dibenzylideneacetone)dipalladium(0) (55mg, 0.06mmol) were added into the mixture in one portion. This mixture was kept stirring for 5h at room temperature, then washed with water and brine. The remaining organic phase was dried over sodium sulfate and all volatile components were removed on a rotary evaporator. Purification by column chromatography (silica gel, 25% DCM in hexanes as eluent) gave the product 4'-bromo-*N*-(4-(methylthio)phenyl)-*N*-phenyl-[1,1'-biphenyl]-4-amine as white solid (615 mg, 1.39 mmol, 69%).  $^1H$ -NMR (400 MHz,  $CD_2Cl_2$ )  $\delta$  7.54 (d,  $J = 8.8$  Hz, 2H), 7.45 (d,  $J = 8.8$  Hz, 4H), 7.28-7.20 (m, 2H), 7.19 (d,  $J = 8.8$  Hz, 2H), 7.11 – 7.02 (m, 7H), 2.47 (s, 3H).  $^{13}C$  NMR (101 MHz,  $CD_2Cl_2$ )  $\delta$  147.82, 147.75, 145.49, 139.90, 133.89, 132.82, 132.16, 129.70, 128.63, 128.52, 127.88, 125.51, 124.77, 123.85, 123.56, 121.14, 16.81. HRMS  $[M+H^+]$   $C_{25}H_{21}BrNS$  Calculated: 446.0578; Found: 446.0564 .

4'-bromo-*N*-(4-(methylthio)phenyl)-*N*-phenyl-[1,1'-biphenyl]-4-amine (320mg, 0.72mmol) and 4,4,4',4',5,5,5',5'-octamethyl-2,2'-bi(1,3,2-dioxaborolane) (91 mg, 0.36 mmol) was added into a 25 mL schlenk flask with 15 mL dried THF, and then the mixture was bubbled with Nitrogen for 20 min. Potassium Carbonate 300 mg was suspended in 1mL water and added into the flask. 5 min

later, Tetrakis(triphenylphosphine)palladium(0) 25 mg (3% eq.) was added under nitrogen atmosphere. The mixture was heated to reflux for overnight. The mixture was cooled to room temperature and then washed with water (50 mL) and brine (50 mL). The remaining organic phase was dried over sodium sulfate, and all volatile components were removed on a rotary evaporator. Purification by column chromatography (silica gel, 25% DCM in hexanes as eluent) gave the product as white solid (162mg, 0.21 mmol, 60%). <sup>1</sup>H-NMR (600 MHz, Acetone-d<sub>6</sub>) δ 7.78 (dd, *J* = 8.5, 7.4 Hz, 8H), 7.67 (d, *J* = 8.4 Hz, 4H), 7.33 (dd, *J* = 8.5, 7.4 Hz, 4H), 7.29 (d, *J* = 8.5, 4H), 7.16 – 7.02 (m, 14H), 2.49 (s, 6H). <sup>13</sup>C-NMR (151 MHz, Acetone-d<sub>6</sub>) δ 147.74, 147.48, 145.38, 139.51, 139.03, 134.50, 132.89, 129.67, 128.40, 127.75, 127.30, 127.03, 125.31, 124.51, 123.73, 123.44, 15.65 HRMS [M<sup>+</sup>] C<sub>50</sub>H<sub>40</sub>N<sub>2</sub>S<sub>2</sub> Calculated: 732.2627; Found: 732.2633.

***N*-(4-(methylthio)phenyl)-*N,N,N'*-triphenyl-[1,1'-biphenyl]-4,4'-diamine (B2-mono)**

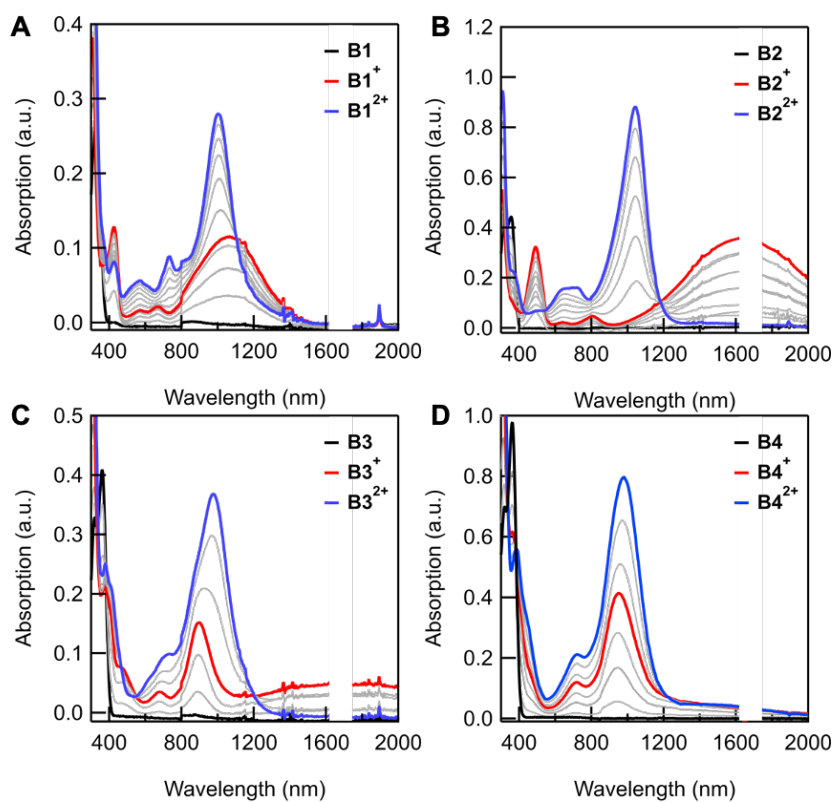


4'-bromo-*N,N*-diphenylbiphenyl-4-amine was synthesized according to literature starting from 4,4'-dibromobiphenyl and diphenylamine, with Pd(OAc)<sub>2</sub>, 1,1'-bis(diphenylphosphino)ferrocene (dppf), and sodium tert-butoxide<sup>1</sup>. 4'-bromo-*N,N*-diphenylbiphenyl-4-amine (78mg, 0.2mmol) and 4-(methylthio)-*N*-phenylaniline (50mg, 0.23mmol) was dissolved in 10mL dry toluene in a 25mL Schlenk tube. Sodium *t*-butoxide (25mg, 0.25mmol) was added into the flask under nitrogen atmosphere and the mixture was stirred for 20 min. Then, tri-*t*-butylphosphine (0.2M, 20μL) and tris(dibenzylideneacetone)dipalladium(0) (5mg, 0.004mmol) were added into the mixture in one portion. This mixture was kept stirring for 5h at room temperature, then washed with water and brine. The remaining organic phase was dried over sodium sulfate, and all volatile components were removed on a rotary evaporator. Purification by column chromatography (silica gel, 25%

DCM in hexanes as eluent) gave the product as white solid (85mg, 0.16mmol, 80%). <sup>1</sup>H-NMR (600 MHz, Methylene Chloride-*d*<sub>2</sub>) δ 7.46 (d, *J* = 8.8 Hz, 4H), 7.31 – 7.23 (m, 6H), 7.19 (d, *J* = 8.6 Hz, 2H), 7.14 – 7.07 (m, 10H), 7.07 – 7.00 (m, 5H), 2.46 (s, 3H). <sup>13</sup>C-NMR (151 MHz, Methylene Chloride-*d*<sub>2</sub>) δ 147.92, 147.74, 147.03, 146.81, 145.55, 134.90, 134.79, 132.23, 129.44, 128.51, 127.38, 125.07, 124.50, 124.35, 124.19, 124.08, 123.08, 16.71. HRMS [M+H<sup>+</sup>] C<sub>37</sub>H<sub>31</sub>N<sub>2</sub>S  
Calculated: 535.2208; Found: 535.2214.

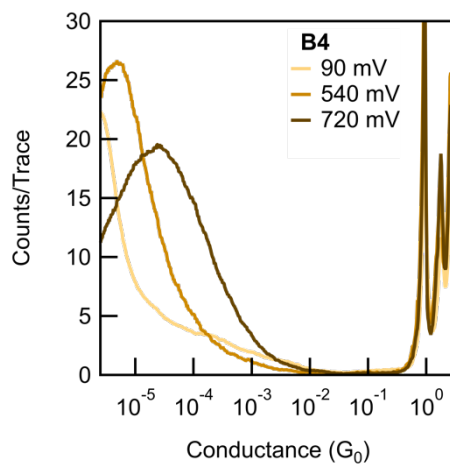
## 2. Oxidative Titration of Bis(triarylamine) Compounds

Oxidative titration of the bis(triarylamine) compounds was conducted in solutions of dichloromethane with concentrations of  $7 \times 10^{-6}$  M for **B1**, and  $1 \times 10^{-5}$  M for both **B2-B4**. 3 mL of these solutions were placed in a UV-Vis cuvette and the one electron oxidant tris(4-bromophenyl)ammoniumyl hexachloroantimonate (BAHA) was added in several steps. The concentration of BAHA solution was  $5 \times 10^{-4}$  M in dichloromethane. Therefore, 42  $\mu$ L of BAHA corresponds to 1 eq of oxidant for **B1**, and 60  $\mu$ L of BAHA corresponds to 1 eq of oxidant of **B2-B4**.

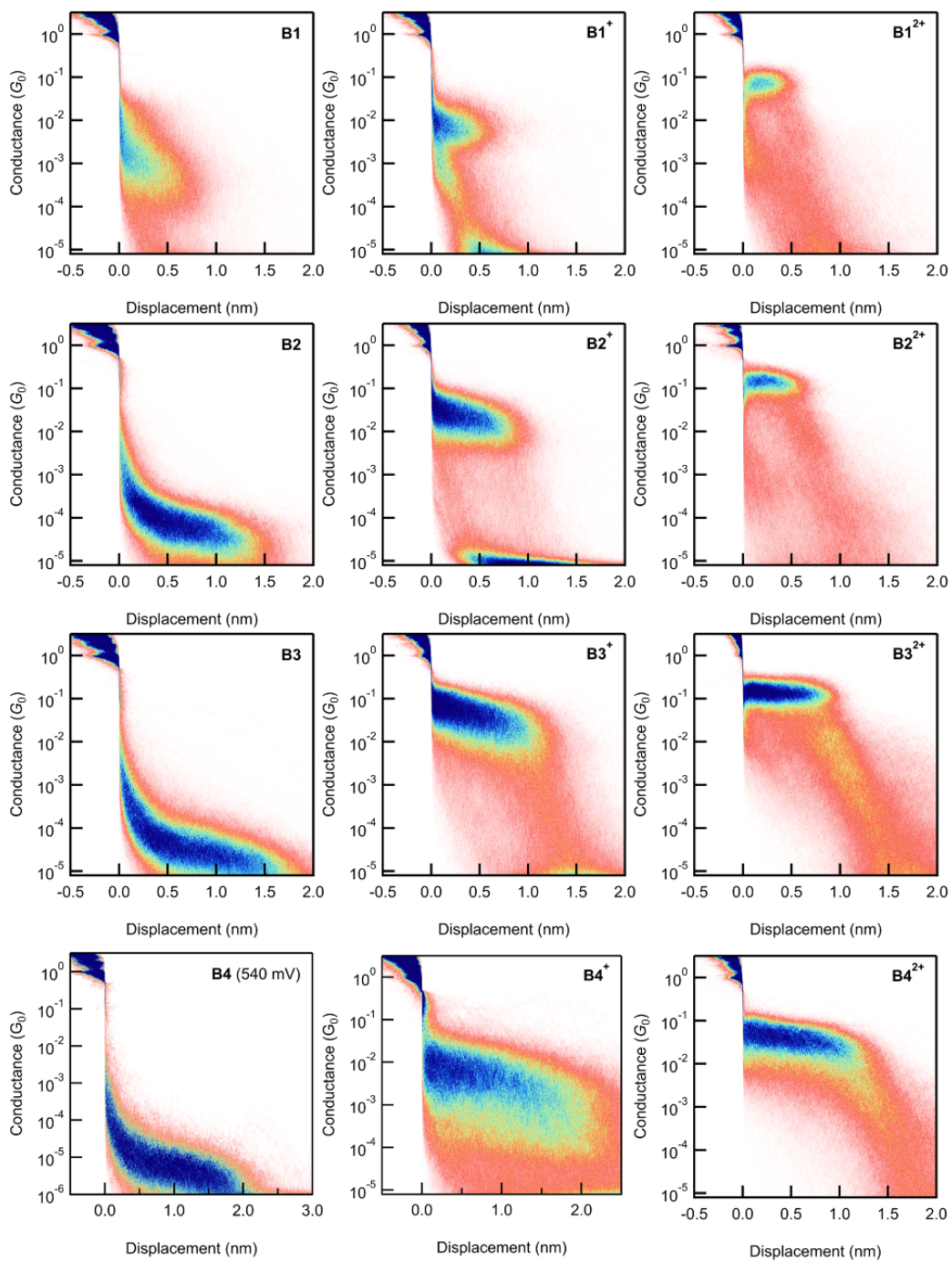


Supplementary Fig. 1. UV-Vis data of oxidative titration of **B1-B4** compounds in dichloromethane, with the spectra of the neutral (black), radical cation (red), and dication (blue) compounds highlighted. The red arrow in (b) shows the direction of peak grown as up to 1 equivalent of BAHA is added, and the blue arrows show peaks that attenuate or grow as the 2<sup>nd</sup> equivalent of BAHA is added.

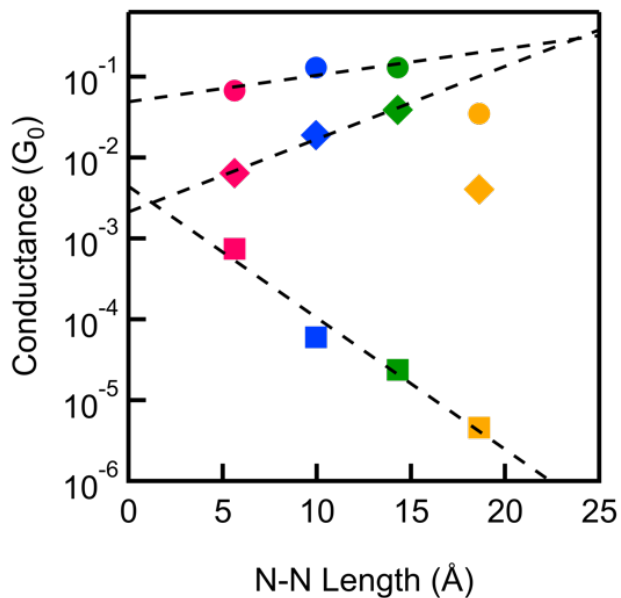
### 3. Additional Conductance Data



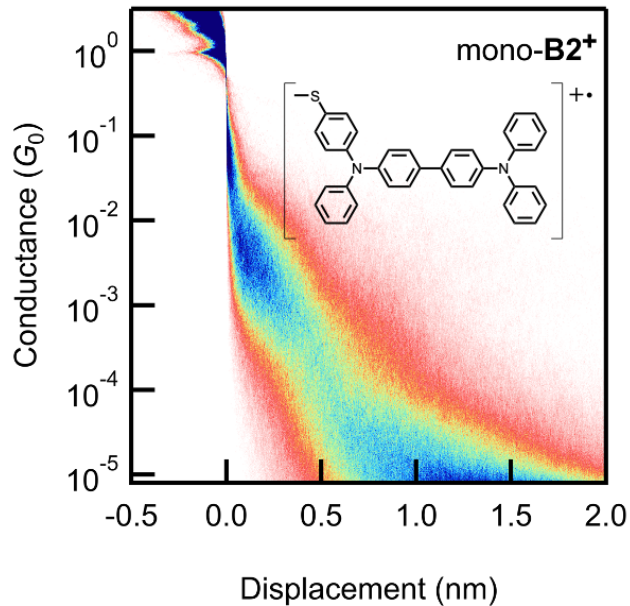
*Supplementary Fig. 2. (a) 1D conductance histograms of **B4** at different applied biases. Note that there is no conductance peak at 90 mV and the feature seen is the noise floor. The bias was therefore increased to 540 mV and 720 mV to confirm whether the molecules were present in the same solution. Clear conductance peaks are seen at these higher biases.*



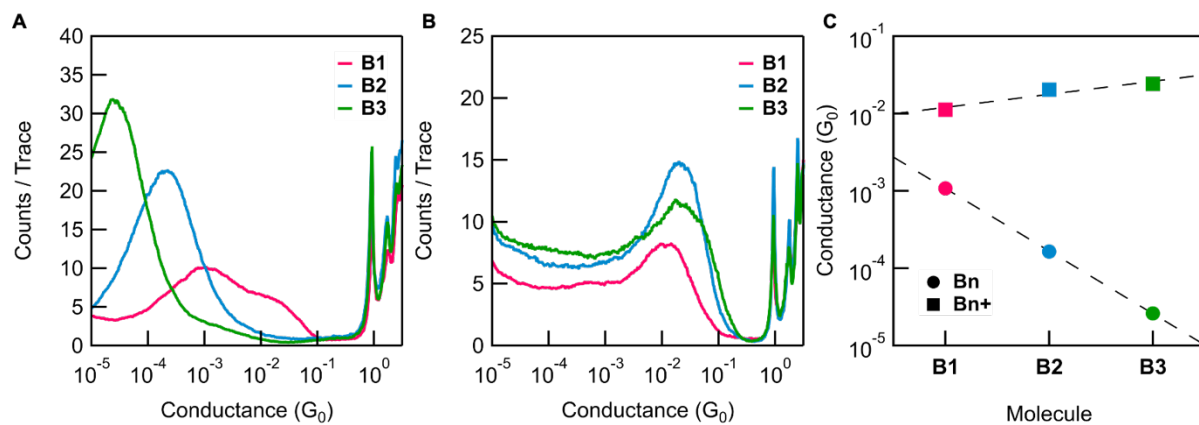
Supplementary Fig. 3. 2D conductance histograms for **B1-B4** (first column), **B1<sup>+</sup>** to **B4<sup>+</sup>** (second column) and **B1<sup>2+</sup>** to **B4<sup>2+</sup>** (third column). Across the series, the plateau lengths increase with increasing molecular length.



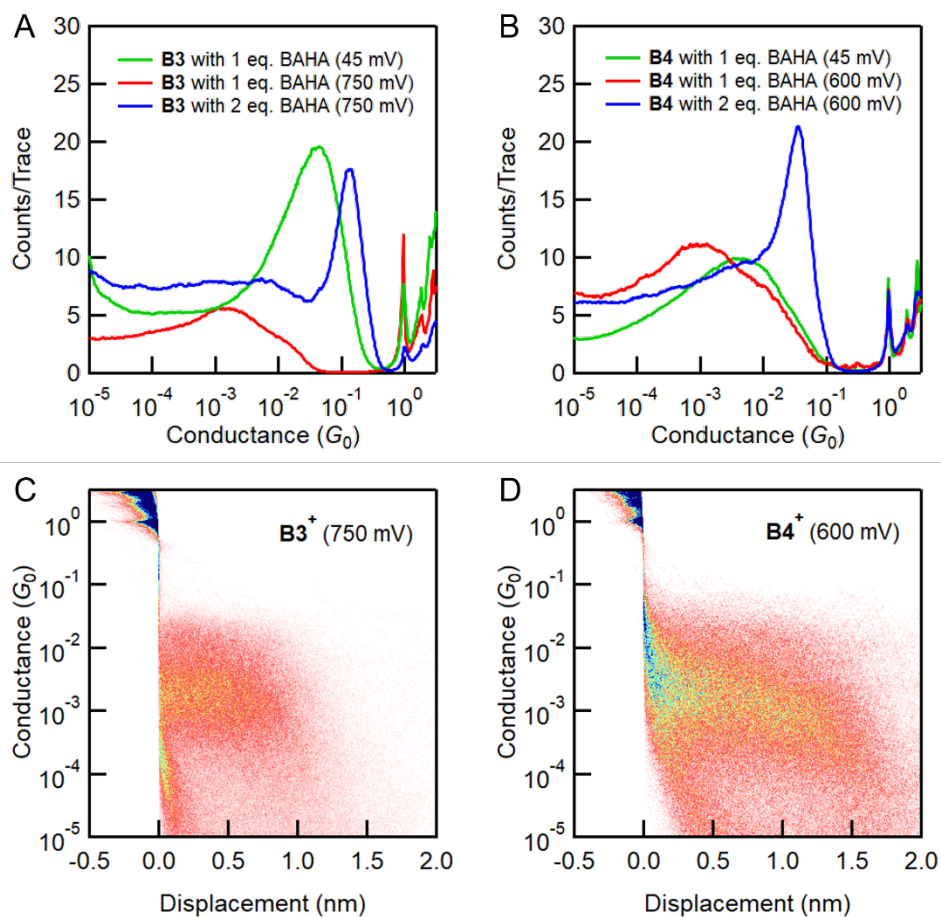
Supplementary Fig. 4. Conductance decay against central chain lengths of **B1-B4** (analogous to Fig. 2D), showing decay constants of  $0.37 \text{ \AA}^{-1}$ ,  $-0.21 \text{ \AA}^{-1}$  and  $-0.07 \text{ \AA}^{-1}$ , respectively. The distance between two nitrogen atoms of **B1-B4** are 5.63, 9.96, 14.29, and 18.62  $\text{ \AA}$ , respectively.



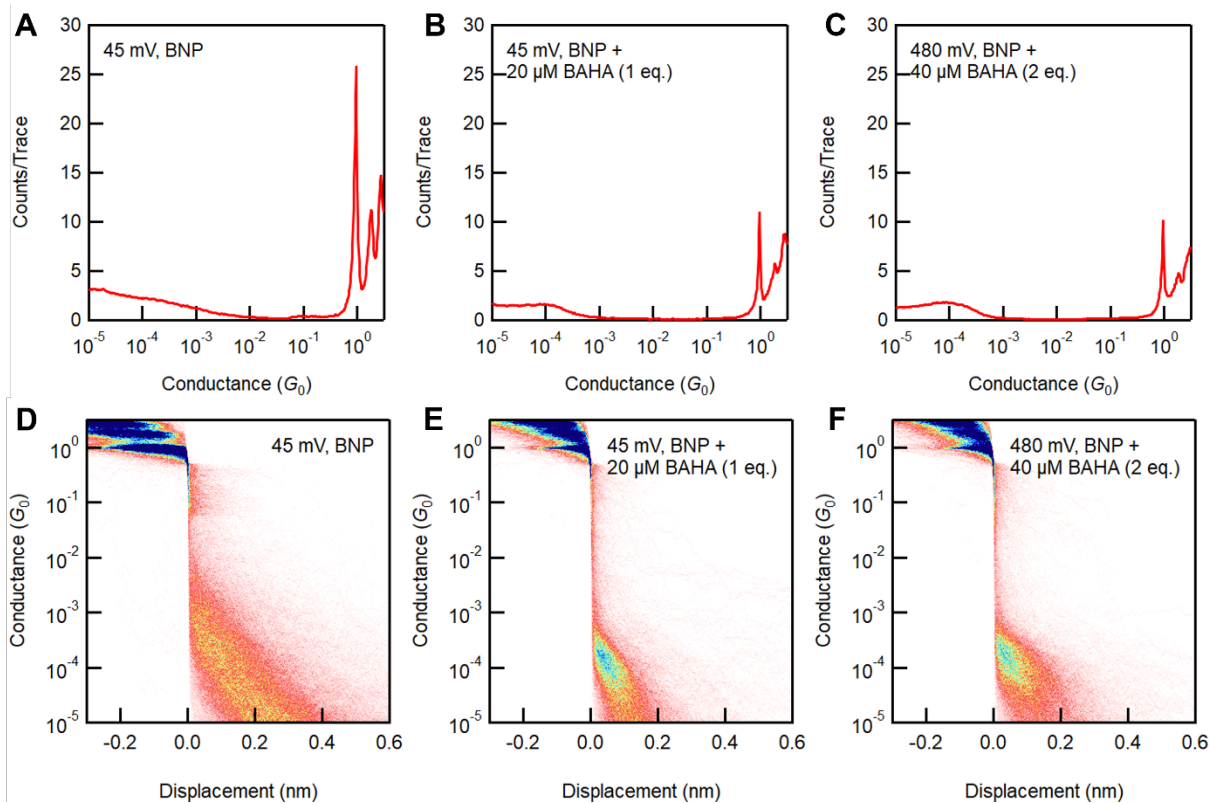
Supplementary Fig. 5. 2D conductance histogram of **mono-B2<sup>+</sup>** that shows no molecular peak.



Supplementary Fig. 6. (A-B) Conductance histograms of **B1-B3** in their (A) neutral state at 90 mV and (B) monocation state at 45 mV in 1,2,4-trichlorobenzene. A larger bias was used for the measurement of the neutral molecules since the histogram peak of **B3** at 45 mV was obscured by the noise floor. (C) Conductance decay of the molecules with increasing length for both states. The  $\beta$  values in trichlorobenzene are 1.9 and -0.4 per phenyl for the neutral and oxidized series respectively.



Supplementary Fig. 7. (A) 1D conductance histograms of **B3** in a 1:3 DCM/BNP mixture with 1 eq. (green, red), and 2 eq. (blue) of BAHA measured at applied biases as indicated in the legend. (B) 1D conductance histograms of **B4** in a 1:3 DCM/BNP mixture with 1 eq. (green, red), and 2 eq. (blue) of BAHA measured at applied biases as indicated in the legend. (C) 2D conductance histograms of the **B3**<sup>+</sup> measurement shown in the red trace in panel (A). (D) 2D conductance histograms of the **B4**<sup>+</sup> measurement shown in the red trace in panel (B).

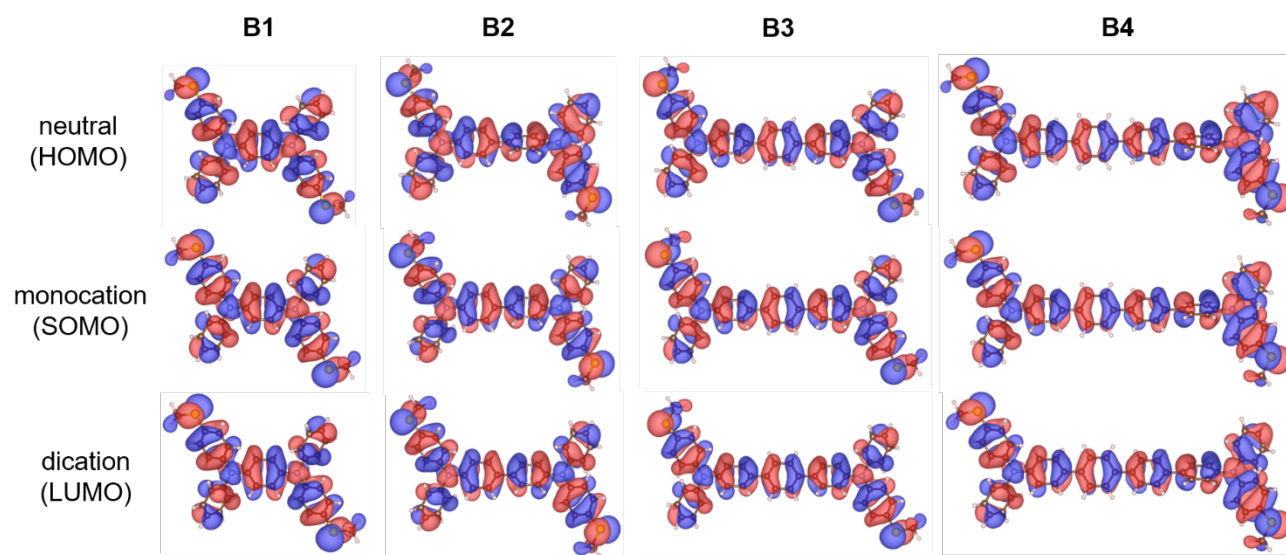


*Supplementary Fig. 8. 1D conductance histograms without molecules measured with (A) BNP as solvent at 45 mV; (B) BNP with 20  $\mu\text{M}$  BAHA in DCM (same as 1 eq. of BAHA in monocation measurements, with DCM:BNP = 1:3), at 45 mV; (C) BNP with 40  $\mu\text{M}$  BAHA in DCM (same as 2 eq. of BAHA in dication measurements, with DCM:BNP = 1:3), at 480 mV. (D-F) Corresponding 2D histograms.*

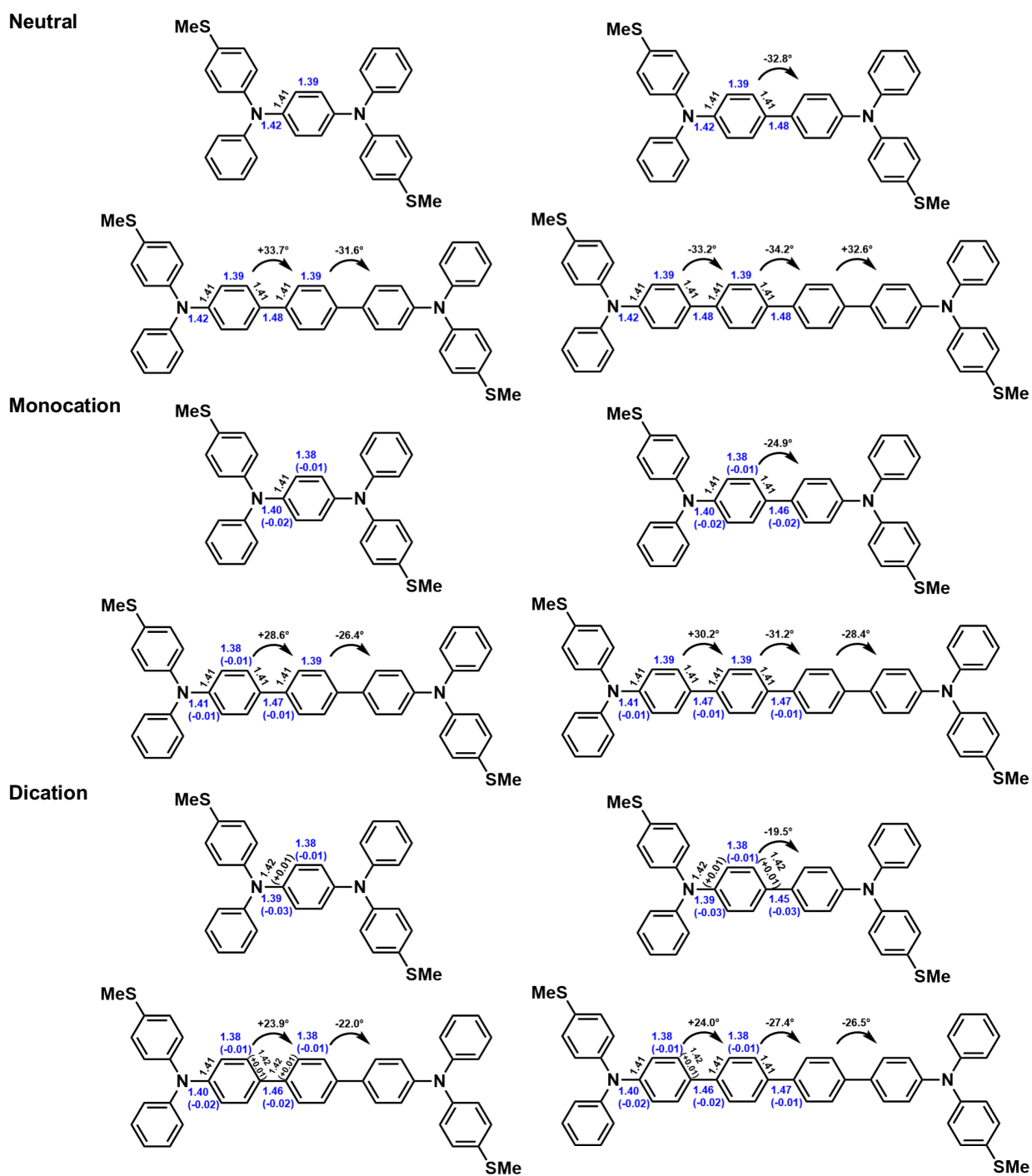
## 4. DFT calculations

Supplementary Table 1. Frontier molecular orbital energies of the neutral, monocation and dication forms of **B1-B4**, in units of eV relative to vacuum.

orbitals	Neutral				Monocation				Dication			
	B1	B2	B3	B4	B1 <sup>+</sup>	B2 <sup>+</sup>	B3 <sup>+</sup>	B4 <sup>+</sup>	B1 <sup>2+</sup>	B2 <sup>2+</sup>	B3 <sup>2+</sup>	B4 <sup>2+</sup>
HOMO-1	-4.68	-4.55	-4.48	-4.46	-7.42	-7.04	-6.76	-6.56	-10.78	-10.20	-9.71	-9.28
HOMO (SOMO for monocation)	-4.13	-4.25	-4.33	-4.37	-6.90	-6.74	-6.59	-6.46	-10.17	-9.54	-9.04	-8.66
LUMO	-1.71	-1.87	-2.08	-2.20	-4.48	-4.51	-4.44	-4.31	-9.70	-9.24	-8.85	-8.55
LUMO+1	-1.56	-1.65	-1.65	-1.66	-4.41	-4.14	-3.87	-3.76	-7.33	-7.14	-6.81	-6.48



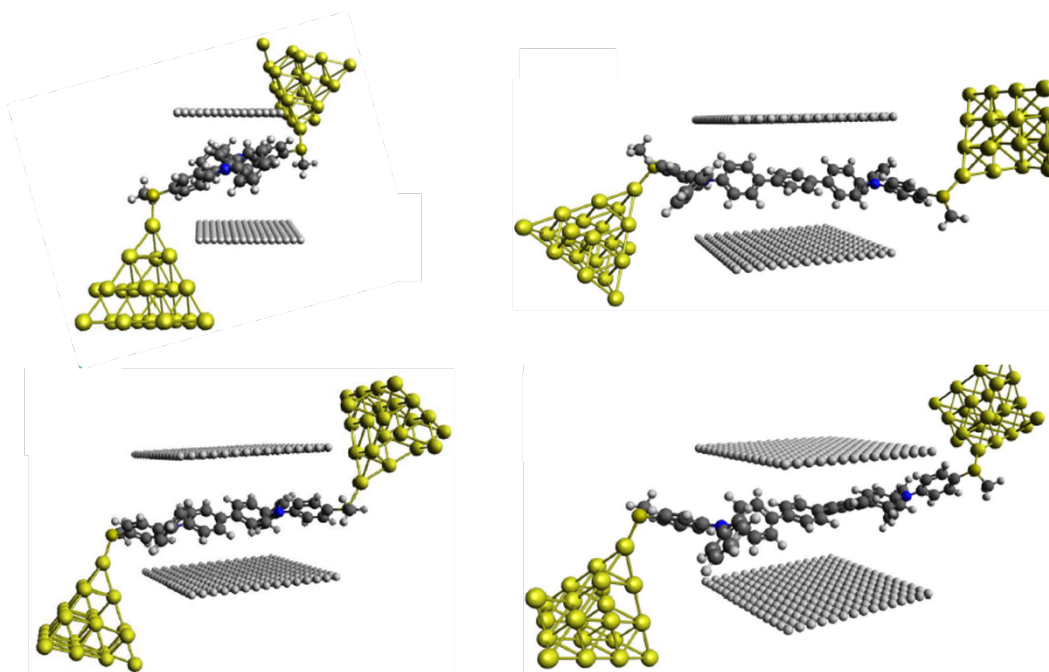
Supplementary Fig. 9. Calculated molecular orbitals of neutral (HOMO), monocation (SOMO) and dication (LUMO) of **B1-B4**.



Supplementary Fig. 10. DFT calculated bond lengths (in unit of Å) and dihedral angles of neutral, monocation and dication series. The values in parentheses are variations from neutral state. All the bonds parallel to the direction of the chains are marked blue.

## Evolution of Bond Lengths from Neutral Molecules to Dications

According to Supplementary Fig. 10, the neutral series has a N–C bond length of 1.42 Å and a C–C bond length between two adjacent phenylenes of 1.48 Å, close to the typical single C–C bond (1.54 Å). This indicates minimal extended conjugation between phenyls. In each phenyl, the C–C bonds that are parallel to the chain are 1.39 Å, slightly shorter than the other four lateral C–C bonds, which are 1.41 Å. After the first oxidation, N–C bonds become shorter (1.40 Å for **B1**<sup>+</sup>, **B2**<sup>+</sup> and 1.41 Å for **B3**<sup>+</sup>, **B4**<sup>+</sup>). Shorter N–C bond length for **B1**<sup>+</sup>, **B2**<sup>+</sup> suggests that they are more delocalized. The bond length of C–C between phenyls is 1.46 Å in **B2**<sup>+</sup> and 1.47 Å in **B3**<sup>+</sup> and **B4**<sup>+</sup>, again indicating some conjugation between the phenyls. For the parallel C–C bonds in phenylenes, the length is 1.38 Å for **B1**<sup>+</sup> and **B2**<sup>+</sup>. In **B3**<sup>+</sup>, the central phenylene has 1.38 Å parallel C–C bonds and two side phenylenes have 1.39 Å bonds, which demonstrates that the delocalization of radical becomes weaker in the center. For **B4**<sup>+</sup>, all the parallel C–C bonds in phenylenes are 1.39 Å, the same as neutral **B4**, which provides further evidence for more localized radical states in **B4**<sup>+</sup>. In the dications, all the N–C bonds are further shortened by 0.01 Å compared with monocations, indicating a stronger delocalization. For **B4**<sup>2+</sup>, the central C–C bond between two phenyls is 1.47 Å, while other two bonds are 1.46 Å, also demonstrating the delocalization is weaker in the central region. For the lateral C–C bonds in phenyls, they are 0.01 Å longer than neutral and monocation series, which supports the formation of quinoidal structures. However, the lateral C–C bond length in the central two phenylenes in **B4**<sup>2+</sup> is close to the neutral case, which demonstrates that it doesn't form an extended quinoid structure.



Supplementary Fig. 11. Geometries of the oxidized **Bn** series in transmission calculations, corresponding to Fig. 4A.

Supplementary Table 2. Mulliken charges of **Bn**<sup>+2+</sup> molecule and electrodes from DFT/PBE calculations for the junctions with geometries shown in Supplementary Fig. 13.

Molecules	Mulliken charge of molecule	Mulliken charge of electrodes
<b>B1</b> <sup>+</sup>	1.035	-0.035
<b>B2</b> <sup>+</sup>	0.946	0.054
<b>B3</b> <sup>+</sup>	0.989	0.011
<b>B4</b> <sup>+</sup>	0.967	0.033
<b>B1</b> <sup>2+</sup>	1.617	0.383
<b>B2</b> <sup>2+</sup>	1.498	0.502
<b>B3</b> <sup>2+</sup>	1.592	0.408
<b>B4</b> <sup>2+</sup>	1.606	0.394

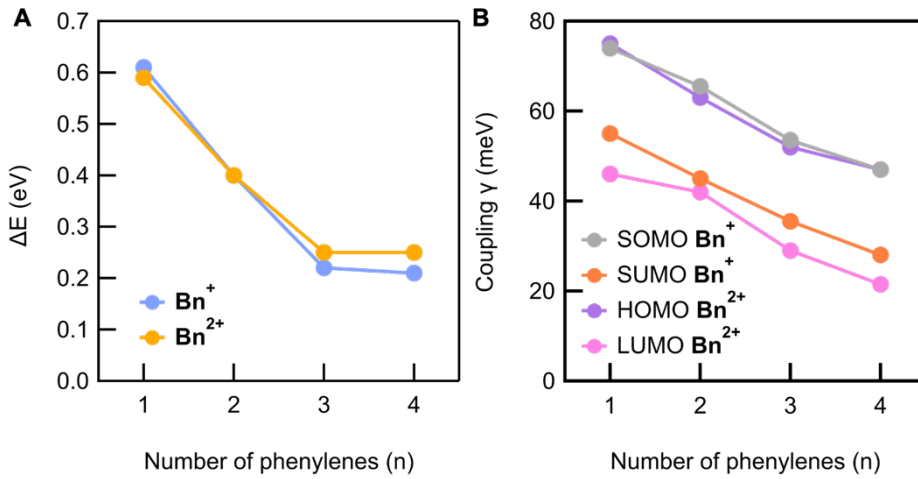
## Obtaining the Transmission Functions

### I. Extracting resonance energies and couplings from the energy-dependent transmission

We fit the three resonances near  $E_F$  in the transmission function  $T(E)$  with the model:

$$T(E) = \left| \sum_{j=1}^3 t_j(E) \right|^2 \text{ where } t_j(E) = e^{i\theta} \frac{\gamma_j}{E - \varepsilon_j + i\gamma_j} \quad \text{Eq. 1.}$$

Here,  $\varepsilon_j$  is the resonance energy and  $\gamma_j$  is the couplings that is obtained from the fit. We report the obtained values for the data from Fig. 4D and 4E in Supplementary Fig. 12.

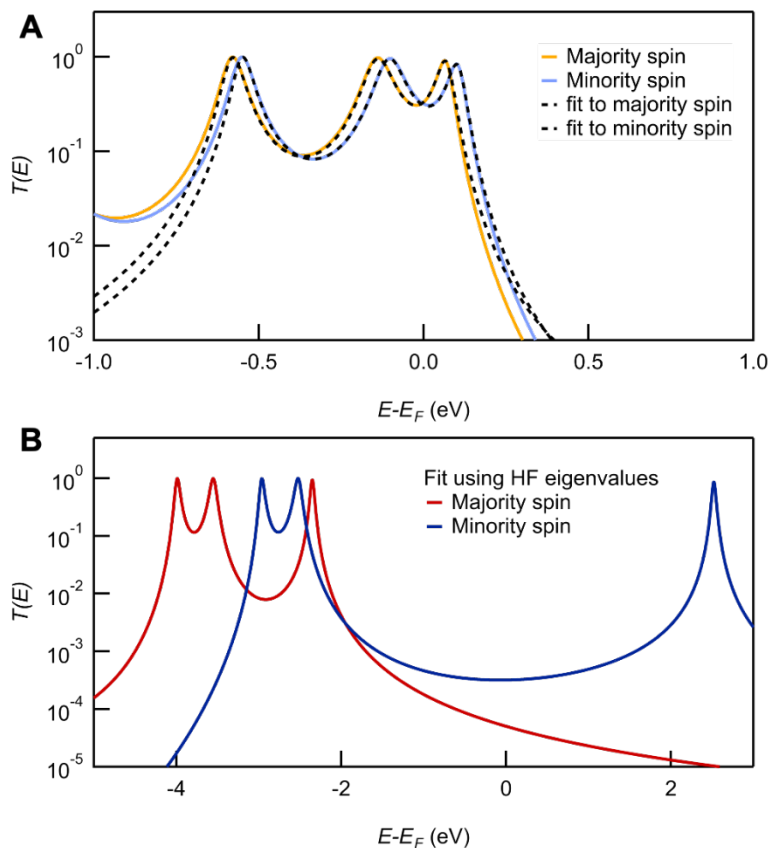


Supplementary Fig. 12. (A) Energy difference ( $\Delta E$ ) of the frontier resonances in the transmission (Fig. 4D and 4E), extracted from fitting  $T(E)$  (Fig. 4D and 4E) to the model in Eq. 1. (B) Couplings  $\gamma_j$  of the frontier peaks in the transmission  $T(E)$  (Fig. 4D and 4E) as extracted from fitting  $T(E)$  to the model above.

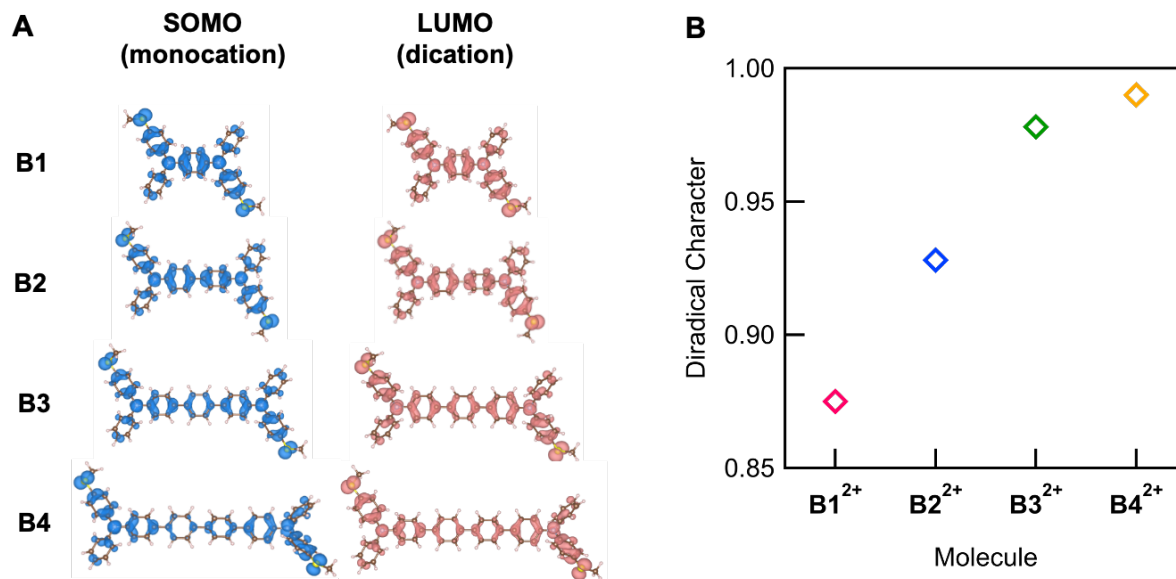
### II. Majority and minority spin contributions in transmission calculations on $Bn^+$ series

Two transmission peaks associated with the frontier orbitals determine the zero-bias conductance  $G = G_0 T(E_F)$  to a large extent, see Supplementary Fig. 13A for the example of  $B4^+$ . For the precise value of  $G$ , the width and the energetic position of both frontier peaks play a key role. We observe that the spin majority and spin minority transmission have very similar shape and are shifted against each other by  $\sim 0.05$  eV on PBE-level – in line with the orbital energies, see Fig. 4B. In a Hartree-Fock-calculation, resonances are shifted further apart, because here non-local exchange is included, so that Coulomb-blockade-type physics is accounted for. This shift has been

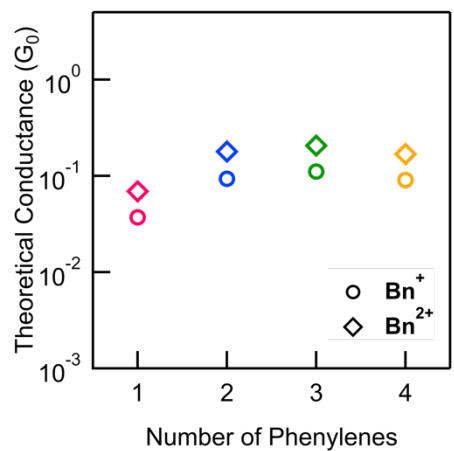
incorporated in the transmission function shown in Supplementary Fig. 13B. As a consequence, the (new) spin-majority transmission peak is narrower as compared to the spin-minority peak, resulting in a negligible contribution of the majority spin to the zero-bias conductance  $G$ . In the main manuscript, we therefore focus on the spin-minority transmission to compute  $G$ .



Supplementary Fig. 13. (A) Transmission of  $\mathbf{B4}^+$  computed from a DFT calculation using the PBE exchange-correlation functional and corresponding fits with Eq. 1. (B) Transmission function for  $\mathbf{B4}^+$  calculated after shifting the three frontier orbitals to the energies determined using Hartree-Fock eigenvalues from Fig. 4C. The contribution to transmission at  $E_F$  from the majority spin channel is small. In the top and bottom figure, the Fermi level has been chosen to be in the middle of the frontier transmission resonances of the spin minority channel.



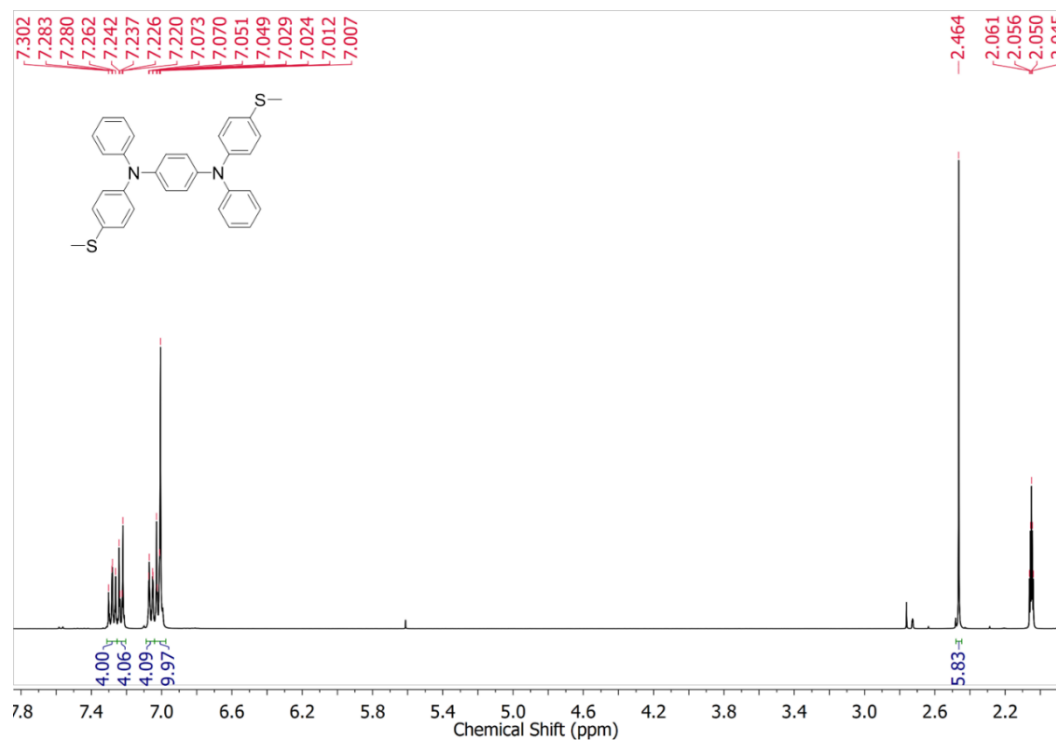
Supplementary Fig. 14. (A) Eigenstate density of SOMO for monocation (blue) and LUMO for dication (red). **B1**<sup>+</sup>-**B3**<sup>+</sup>, and **B1**<sup>2+</sup>-**B3**<sup>2+</sup> feature delocalized orbitals over the whole molecule, which provide further evidence for coupled radical states. The eigenstate density in **B4** shows decrease of amplitude in central region for both monocation and dication forms, which sequesters the coupling to the two sides of the molecule, leading to preferred localized open-shell radical and diradical states. This localization hampers electron transmission, which explains the decrease in conductance for both **B4**<sup>+</sup> and **B4**<sup>2+</sup> when compared with their shorter analogs. (B) Diradical character of the isolated **B1**<sup>2+</sup>-**B4**<sup>2+</sup> calculated using DFT. The diradical character increases from **B1**<sup>2+</sup> to **B4**<sup>2+</sup> but the change from **B3**<sup>2+</sup> to **B4**<sup>2+</sup> is small.



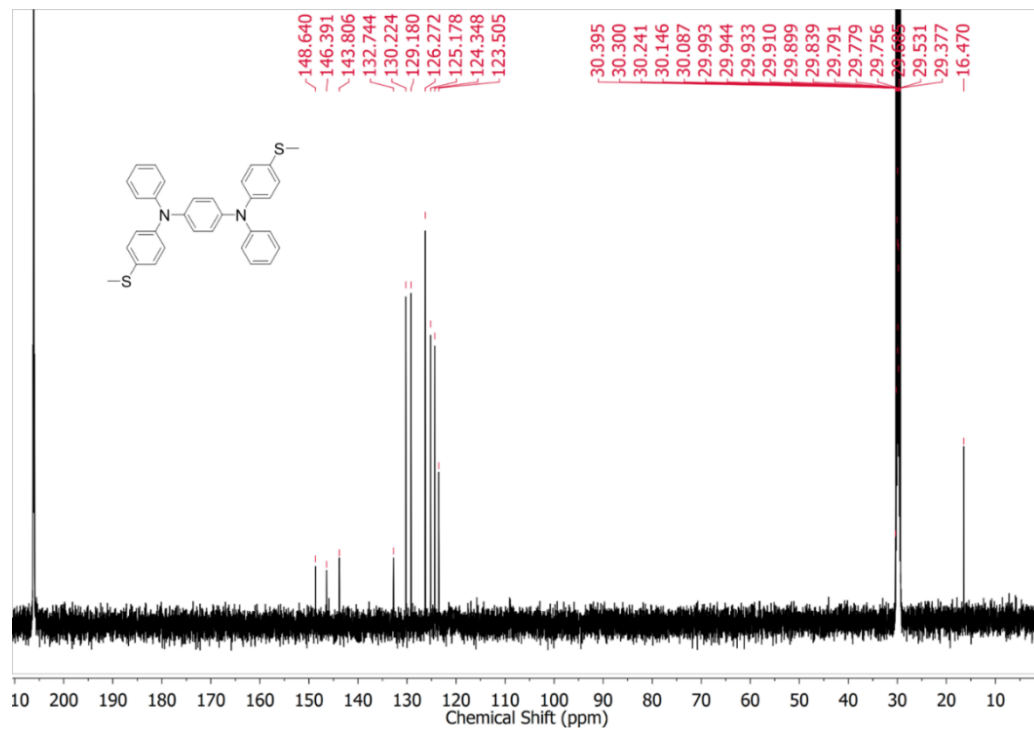
Supplementary Fig. 15. Conductance values of monocations and dicationic species obtained by integrating the calculated transmission function over 0.4 eV bias window that is opened symmetrically about the Fermi energy. The conductance trends follow:  $B1 < B2 < B3 > B4$  for both series.

## 5. NMR Spectra

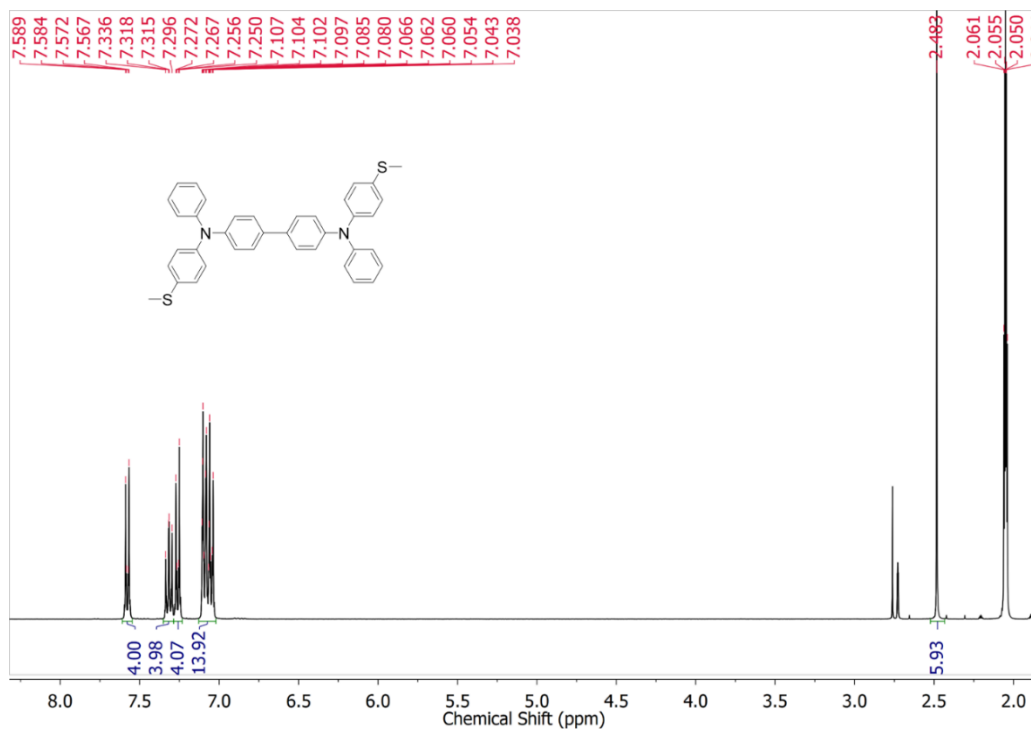
$^1\text{H-NMR}$  of **B1** (400 MHz, Acetone- $d_6$ , 25°C)



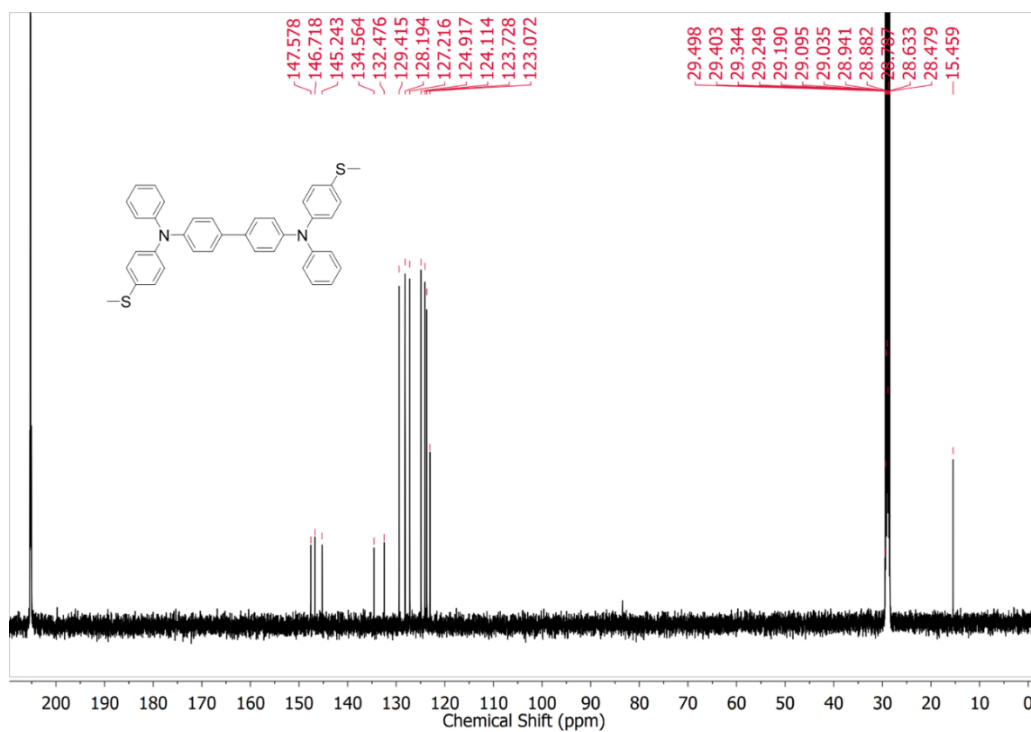
$^{13}\text{C-NMR}$  of **B1** (500 MHz, Acetone- $d_6$ , 25°C)



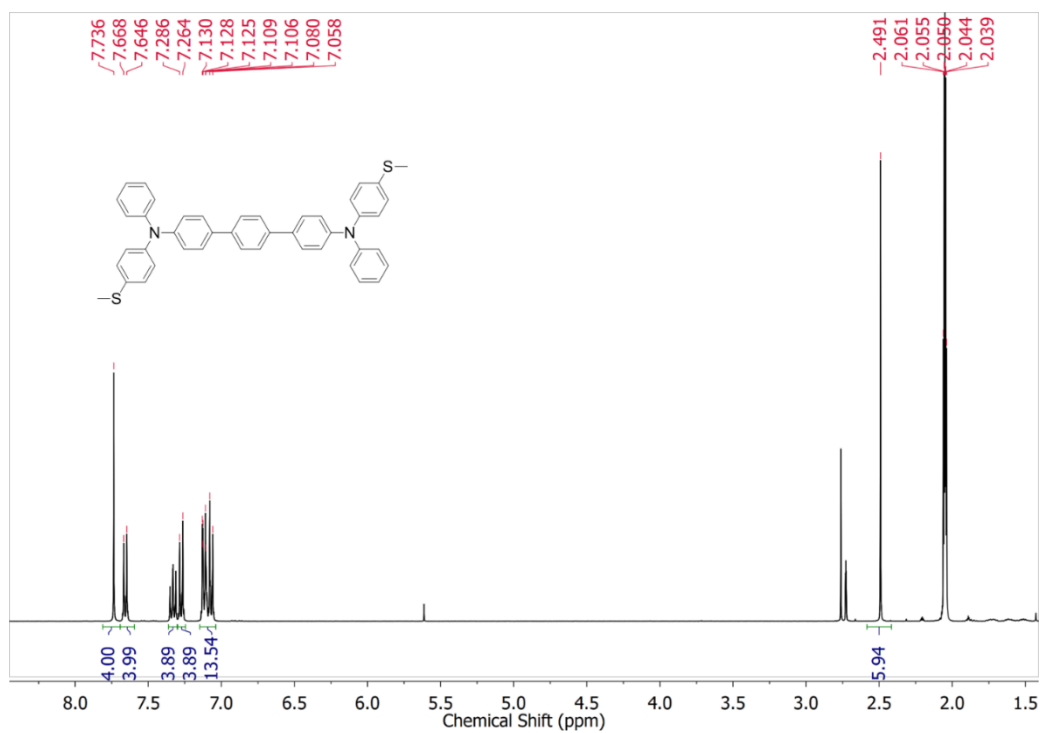
<sup>1</sup>H-NMR of **B2** (400 MHz, Acetone-d<sub>6</sub>, 25°C)



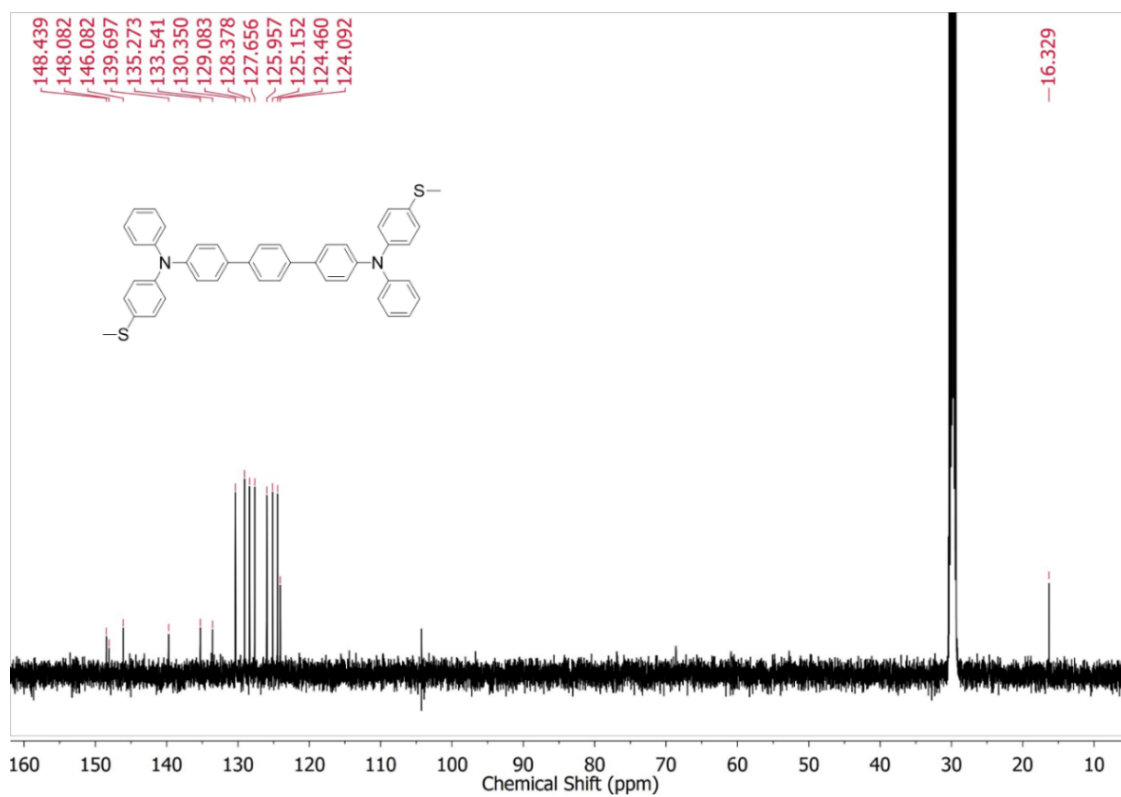
<sup>13</sup>C-NMR of **B2** (500 MHz, Acetone-d<sub>6</sub>, 25°C)



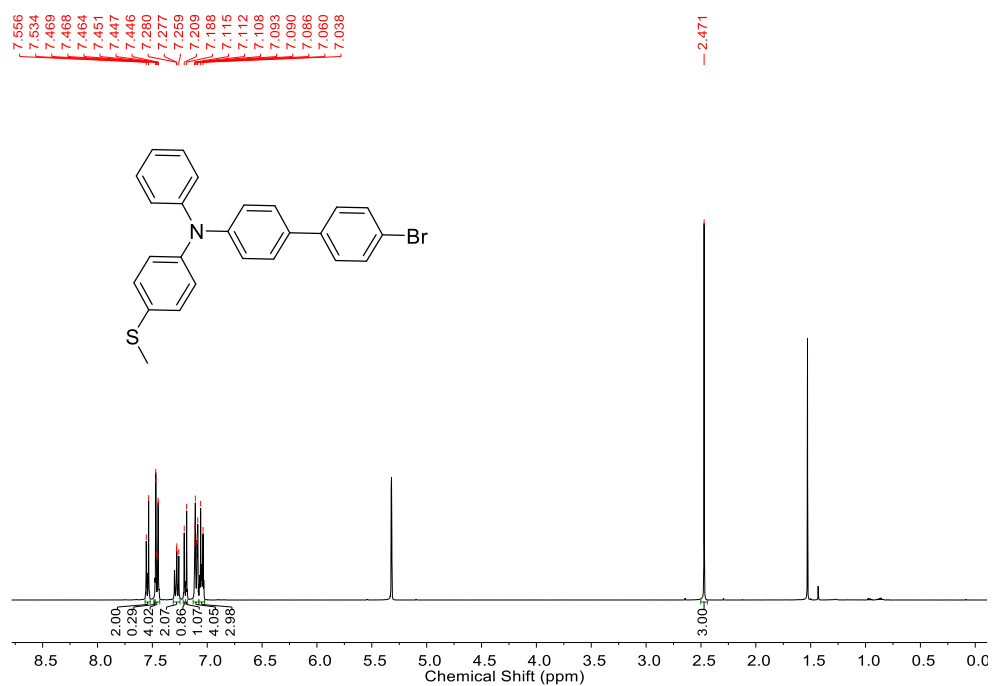
$^1\text{H-NMR}$  of **B3** (400 MHz, Acetone- $d_6$ , 25°C)



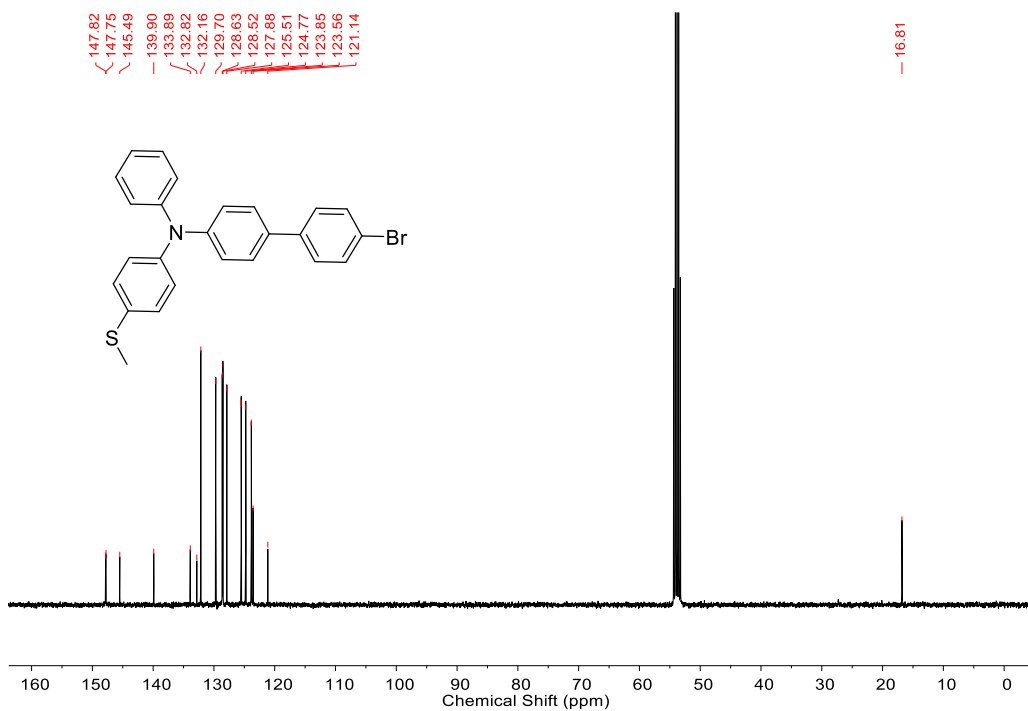
$^{13}\text{C-NMR}$  of **B3** (500 MHz, Acetone- $d_6$ , 25°C)



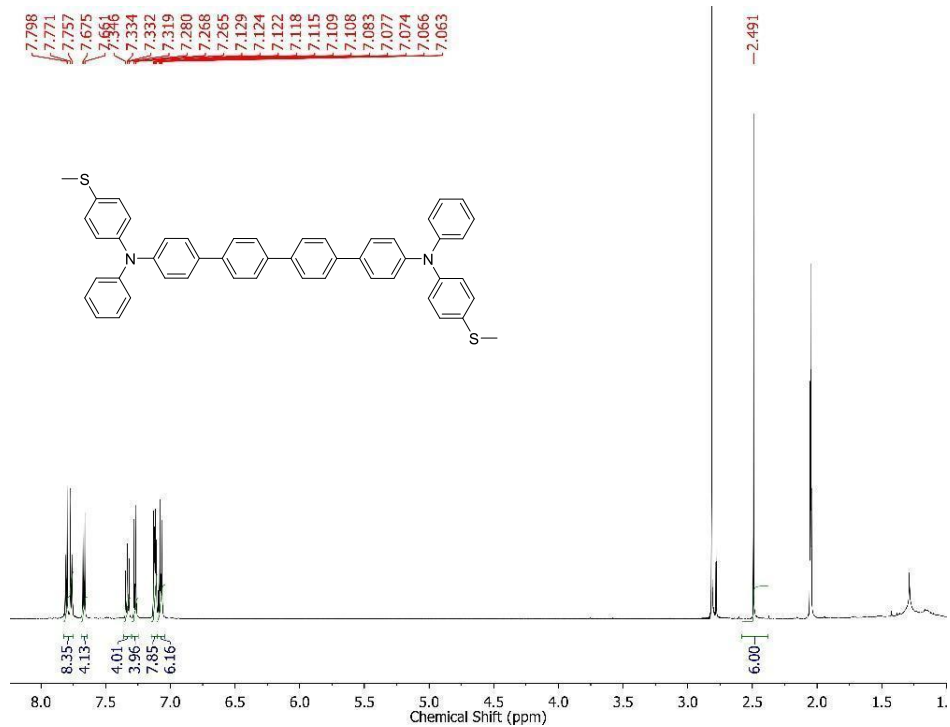
<sup>1</sup>H-NMR of 4'-bromo-N-(4-(methylthio)phenyl)-N-phenyl-[1,1'-biphenyl]-4-amine (400 MHz, Acetone-d<sub>6</sub>, 25°C)



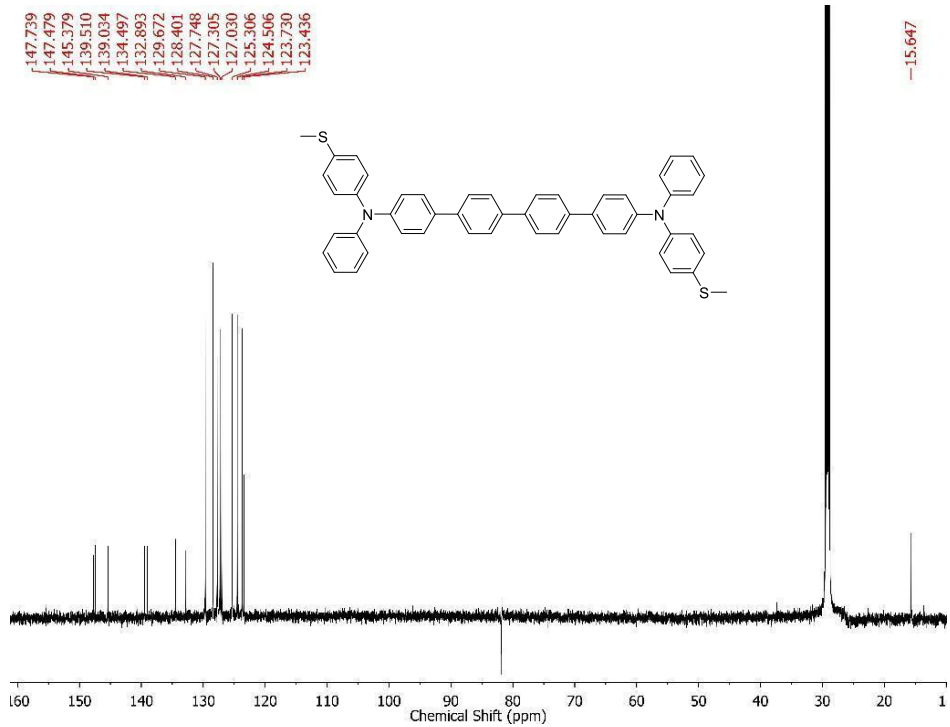
<sup>13</sup>C-NMR of 4'-bromo-N-(4-(methylthio)phenyl)-N-phenyl-[1,1'-biphenyl]-4-amine (400 MHz, Acetone-d<sub>6</sub>, 25°C)



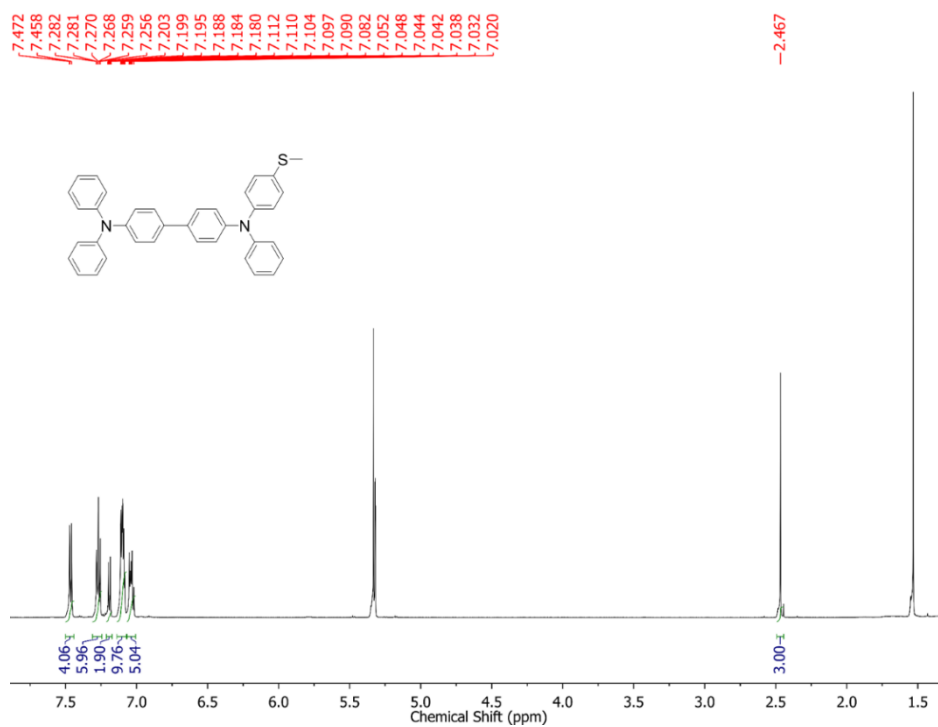
<sup>1</sup>H-NMR of **B4** (400 MHz, Acetone-d<sub>6</sub>, 25°C)



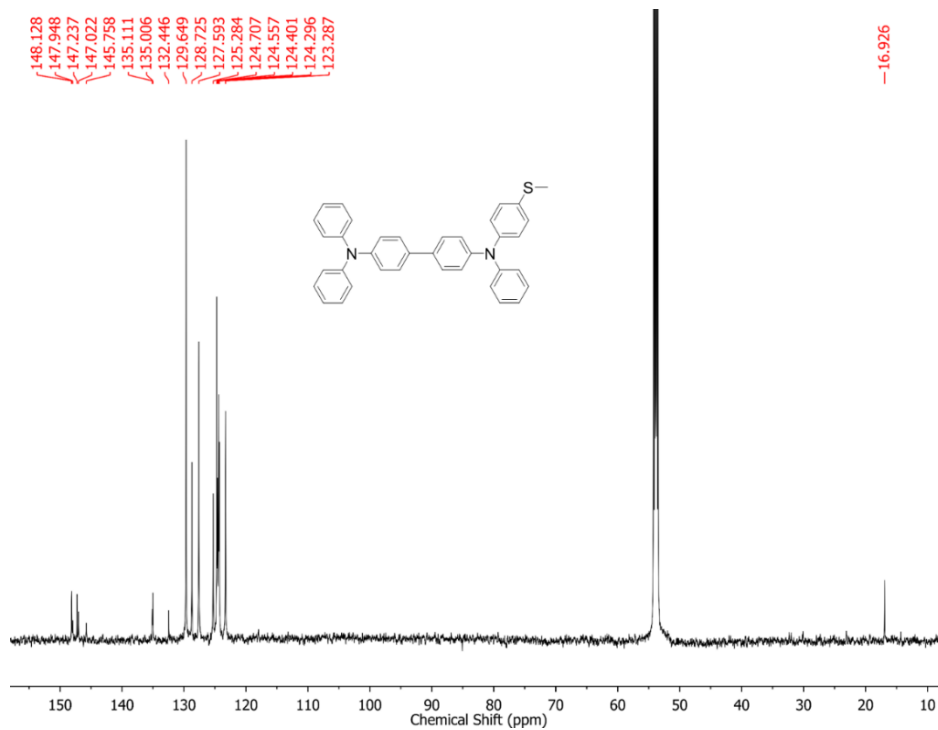
<sup>13</sup>C-NMR of **B4** (500 MHz, Acetone-d<sub>6</sub>, 25°C)



<sup>1</sup>H-NMR of **mono-B2** (400 MHz, CD<sub>2</sub>Cl<sub>2</sub>, 25°C)



<sup>13</sup>C-NMR of **mono-B2** (500 MHz, CD<sub>2</sub>Cl<sub>2</sub>, 25°C)



## 6. References

- 1 Chen, Z. *et al.* High performance exciplex-based fluorescence–phosphorescence white organic light-emitting device with highly simplified structure. *Chemistry of Materials* **27**, 5206-5211 (2015).
- 2 Datta, S. *Electronic transport in mesoscopic systems.* (1995).
- 3 Scheer, E. & Cuevas, J. C. *Molecular electronics: an introduction to theory and experiment.* Vol. 15 (World Scientific, 2017).